

Formation of medium-range order clusters in Al-Ni-Ce amorphous and liquid alloys

This article has been downloaded from IOPscience. Please scroll down to see the full text article.

2002 J. Phys.: Condens. Matter 14 1163

(<http://iopscience.iop.org/0953-8984/14/6/305>)

View [the table of contents for this issue](#), or go to the [journal homepage](#) for more

Download details:

IP Address: 171.66.16.27

The article was downloaded on 17/05/2010 at 06:08

Please note that [terms and conditions apply](#).

Formation of medium-range order clusters in Al–Ni–Ce amorphous and liquid alloys

Zhao Fang, Wu Youshi¹, Zhang Chuanjiang, Zhu Zhiqian, Shi YuanChang and Zhou Guorong

College of Materials Science and Engineering, Shandong University (South Campus), Jinan 250061, Shandong Province, People's Republic of China

E-mail: wysfmx@jn-public.sd.cninfo.net

Received 21 July 2001, in final form 22 October 2001

Published 1 February 2002

Online at stacks.iop.org/JPhysCM/14/1163

Abstract

The small-angle information in the total structure factors and x-ray diffraction pattern have been investigated. Prepeaks were found to exist in the total structure factors in the Al₉₀Ni₅Ce₅ liquid and amorphous alloys. The prepeak position is almost the same in the liquid alloys at different temperatures and are nearly identical when the liquid alloys were quenched to the amorphous state. The medium-range order clusters are formed in the liquid state and the structural unit can be preserved to the amorphous state. The amorphous Al₉₀Ni₅Ce₅ alloys crystallize in two stages. The first stage corresponds to the precipitation of face-centred-cubic Al and in the second crystallization stage intermetallic compounds are formed. The structure corresponding to the prepeak is preserved, and even strengthened, during rapid solidification, but is not stable and decomposes at room temperature. The structural unit is like a large atom during rapid solidification, which may be the reason for the high glass forming ability in Al–Ni–Ce systems.

1. Introduction

It has been known that the amorphization of metallic materials causes a remarkable increase in mechanical properties [1]. The amorphous alloys in Al–TM–RE systems with aluminium content up to 90 at.% have been found to have high mechanical strength and good ductility [2, 3]. Furthermore, it has been found that Al-based Al–Ni–RE amorphous alloys containing face-centred-cubic (fcc) Al particles exhibit further improved tensile fracture strengths combined with good bending ductility as compared with those for the amorphous single-phase alloys with the same composition [4]. However, the other ternary Al–TM–RE amorphous alloys containing fcc Al particles was found to be brittle when the TM is a transition metal such as Mn, Fe or Co and these alloys were found to be ductile when the TM is a mixture with Ni in some

¹ Author to whom any correspondence should be addressed.

compositional range [5]. Usually, the formation of nanocrystals with excellent mechanical properties in Al-based alloys is not made directly by quenching but rather by overquenching to generate a fully amorphous state and thus the glass phase is then partially devitrified to produce a nanometre-scale dispersion of Al crystallites in a glassy matrix [6]. In case of the ternary Al–Ni–Y glasses, the formidable tensile strength often exceeds 800 MPa or 1 GPa [7]. It is necessary to study the glassy state so as to explain the transformation from a glassy state to a nano-crystalline state [6]. The atomic structure has been investigated in order to explain the unusual glass forming ability in Al-based alloys [8–11]. These studies have mainly focused on the main peak of the statistical function, or the radial distribution function (RDF) of the amorphous alloys, which cannot reflect the strong local compositional and geometrical order [12]. The small-angle information in Al–Ni–Ce systems is often ignored. The formation of metallic glasses by the melt spinning technique is strongly dependent on the processing parameters. One of the most important technical parameters is the quenching temperature, which can modify the viscosity of the melts [13]. However, the effects of the liquid structure on the amorphous structure are often ignored. In our investigation, the prepeak was found both in the total structure factors of liquid and amorphous Al–Ni–Ce alloys. In this paper, we investigated the small angle information in Al–Ni–Ce systems and the effects of the chemical short-range order structure in the liquid alloys on the amorphous Al–Ni–Ce alloys. We also discussed the thermal stability and the high glass forming ability of the Al–Ni–Ce amorphous alloys.

2. Experiments

Ingots of Al–Ni–Ce alloys with nominal composition were prepared by arc melting the mixture of high purity Al, Ni and Ce in an argon atmosphere. Amorphous ribbons were prepared by a single-roller melt-spinning technique under a partial argon atmosphere. The diameter of the copper roller was 35 cm, with a typical circumferential velocity of 40 m s⁻¹. The ribbons were ~2 mm in width and ~25 μm in thickness.

The structure of the ribbon samples and liquid alloys was examined by x-ray wide-angle diffraction (XRD) with Cu K α radiation (Mo K α for liquid alloys). The liquid specimens were prepared in a crucible made of Al₂O₃ of size 8 × 25 × 30 mm³ in a high purity helium atmosphere. Measurements were carried out with an accuracy of ±5 °C. The x-ray scattering intensity from liquid alloys was measured using a θ – θ diffractometer which allows the sample to be held in a stationary horizontal position and the x-ray tube and detector moved in opposite directions. As shown in figure 1, the prepeak is observed in the XRD pattern. The scattering intensity measured in arbitrary units can be converted into the coherent scattering intensity per atom in electron units, using the generalized Krogh–Moe–Norman method [14] with the atomic scattering factor including the anomalous dispersion factor [15]. Compton scattering is also corrected using the values given by Cromer and Mann [16]. Then, the total structure factor $S(Q)$ can be obtained from the scattering intensity, where $Q = 4\pi \sin \theta / \lambda$ is the magnitude of the scattering vector and λ is the wavelength [14]. A parabolic-like function $f(x) = ax^2 + bx^3$, in which b is often much smaller than a , was used to fit the small-angle part of $S(Q)$. Separation of the prepeak is executed by $S(Q)$ minus the fit function [17].

Thermal analysis was performed using a Netzsch DSC-404 system under a pure argon atmosphere.

3. Results

The total structure factors of liquid Al₉₀Ni₅Ce₅ alloys at different temperatures are shown in figure 2. The intensity of the main peak decreases as temperature increases, as expected for greater disorder. The most intriguing feature is the existence of the prepeak, which has

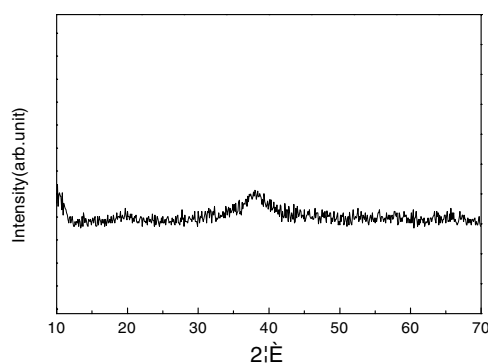


Figure 1. The XRD pattern of amorphous $\text{Al}_{90}\text{Ni}_5\text{Ce}_5$ alloys quenched at 1300°C .

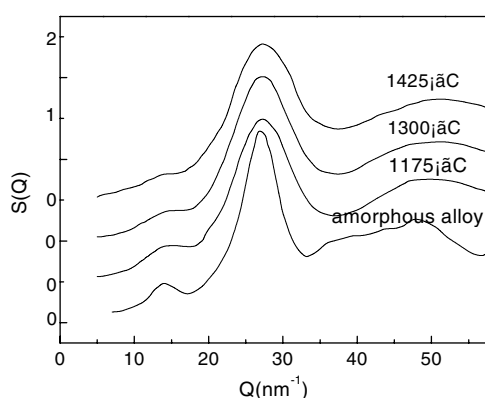


Figure 2. Total structure factors of liquid $\text{Al}_{90}\text{Ni}_5\text{Ce}_5$ alloys at different temperatures and amorphous $\text{Al}_{90}\text{Ni}_5\text{Ce}_5$ alloys quenched at 1300°C .

been found at all temperatures investigated. The positions of the main peak remain almost at a constant value around 27.2 nm^{-1} . The statistic error in the position of the peak has been evaluated by the method developed by Egami [18] and the error in the position of the prepeak is relatively large due to its broad shape. The positions of the prepeak remain nearly around a constant value of 14 nm^{-1} at different temperatures. From figure 2, it can also be seen the prepeak intensity decreases with increasing temperature.

The total structure factors of amorphous $\text{Al}_{90}\text{Ni}_5\text{Ce}_5$ alloys quenched at 1300°C are also shown in figure 2. The main peak is located at around 27.2 nm^{-1} . It can also be seen that a prepeak exists in the structure factors of amorphous alloys. The prepeak position is 14.0 nm^{-1} , with the statistic error $\pm 0.5 \text{ nm}^{-1}$. The prepeak in the amorphous alloys has almost the same position as that of the liquid alloys.

The repetitive characteristic distance R is usually estimated by using the equation $R = 2\pi/Q_p$, where Q_p is the prepeak position and the correlation length can be estimated using a simple expression $D \approx 2\pi/\Delta Q$, where ΔQ is the half width of the prepeak [12, 19]. ΔQ is obtained after separating the prepeak by the parabolic-like function [17]. Table 1 shows characteristic periodicity R , half width of the prepeak ΔQ and the correlation length D of liquid alloys at different temperatures and the amorphous alloys quenched at 1300°C corresponding to the prepeak. The correlation length increases with decreasing temperature

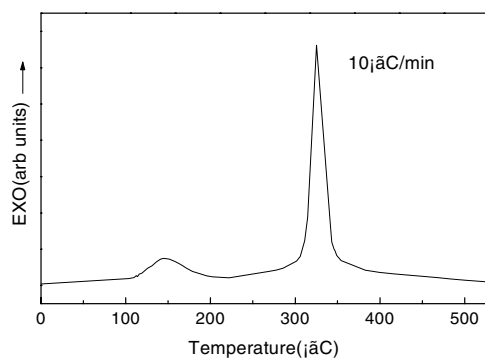


Figure 3. DSC curves of amorphous $\text{Al}_{90}\text{Ni}_5\text{Ce}_5$ alloys quenched at $1300\text{ }^\circ\text{C}$.

Table 1. Characteristic periodicity R , half width of the prepeak ΔQ and the correlation length D of liquid and the amorphous $\text{Al}_{90}\text{Ni}_5\text{Ce}_5$ alloys quenched at $1300\text{ }^\circ\text{C}$.

Temperature ($^\circ\text{C}$)	Liquid alloy			Amorphous alloy		
	R (nm)	ΔQ (nm^{-1})	D (nm)	R (nm)	ΔQ (nm^{-1})	D (nm)
1175	0.449	5.4	1.14			
1300	0.446	6.1	1.03	0.449	3.5	1.80
1425	0.449	7.0	0.90			

in liquid $\text{Al}_{90}\text{Ni}_5\text{Ce}_5$ alloys. However, the correlation length of the amorphous alloys is much larger than that of the liquid alloys.

In order to examine the thermal stability and the crystallization process, differential scanning calorimetry (DSC) were performed. Figure 3 shows the DSC curves of amorphous $\text{Al}_{90}\text{Ni}_5\text{Ce}_5$ alloys quenched at $1300\text{ }^\circ\text{C}$. Two exothermic peaks are observed. The first exothermic peak is very weak at low temperatures and no glass transition is found. The second peak is at high temperatures with a strong exothermic peak.

In order to trace the crystallization process, XRD patterns at different temperatures were also examined. Figures 4 (a), (c) and (d) show the XRD patterns at different temperatures of the amorphous $\text{Al}_{90}\text{Ni}_5\text{Ce}_5$ alloys. At ambient temperature, the XRD pattern indicates that the as-quenched ribbons are amorphous and a prepeak is found at $2\theta = 20^\circ$. At $240\text{ }^\circ\text{C}$, after the first crystallization peak, the prepeak disappears and the fcc Al phase appears. At $360\text{ }^\circ\text{C}$, several intermetallic compounds indicated as Al_3Ni and $\text{Al}_{11}\text{Ce}_3$ phases are formed. A similar two-stage crystallization process has been reported for $\text{Al}_{90}\text{Fe}_5\text{Ce}_5$ alloys by Dunlap *et al* [20]; figure 4(b) shows the XRD patterns of the amorphous alloys that were stored at room temperature for 3 months. The fcc Al phase appears and the prepeak becomes more diffuse and weak.

4. Discussion

The presence of the prepeak provides evidence of the atomic ordering extending beyond the first-neighbour shell [21] and extending over to medium-range order [22–24]. As shown in table 1, the correlation length of the liquid and amorphous $\text{Al}_{90}\text{Ni}_5\text{Ce}_5$ alloys corresponding to the prepeak is in the medium-range order scale (0.5–2 nm). The medium-range order is caused by regularities in the packing of structural units [24]. The correlation length corresponding

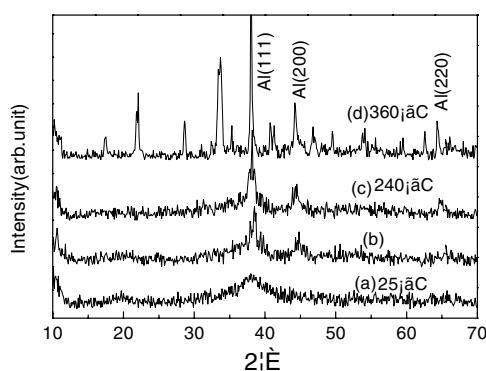


Figure 4. (a), (c) and (d) XRD patterns at different temperatures of the amorphous $\text{Al}_{90}\text{Ni}_5\text{Ce}_5$ alloys. (b) XRD patterns of the amorphous alloys that were stored at room temperature for 3 months.

to the prepeak reflects the cluster size and each cluster contains several basic structural units with chemical short-range order [12,25]. The structural unit size corresponding to the prepeak can be estimated according to equation used for calculating the characteristic periodicity, $R = 2\pi/Q_p$ [12,25,26]. Therefore, the characteristic structural unit size can be obtained from table 1. As shown in figure 2, the prepeak is located at almost the same position at different temperatures in the liquid alloys. The same prepeak position implies that the structural unit has the same size or the same characteristic periodicity in real space in the medium-range order cluster. It indicates that the structural unit corresponding to the prepeak is the same at the different temperatures in the liquid alloys. From figure 2, one can see that the prepeak in the amorphous alloys has the same position as that in the liquid alloys. This is evidence that the structural unit in the amorphous alloys is the same as that in the liquid alloys. Therefore, the structural unit in the liquid alloys can be preserved to the amorphous state.

From figure 4, it can be seen that the prepeak disappears and the fcc Al phase precipitates from the amorphous matrix after crystallization past the first exothermic peak. This indicates that the structure corresponding to the prepeak is not stable in the solid state and can easily decompose. However, at this crystallization stage, no evidence of any diffraction peaks appears at the position of the prepeak. It is a sign that the structure corresponding to the prepeak cannot be as the nuclei of a metastable phase. However, the structure corresponding to the prepeak exists in the liquid alloys. Therefore, the structure corresponding to the prepeak is formed in the liquid.

As shown in table 1, the correlation length of the liquid and amorphous $\text{Al}_{90}\text{Ni}_5\text{Ce}_5$ alloys corresponding to the prepeak, or the cluster size, varies with liquid temperature or the quenching temperature. In the liquid alloys, while the temperature is increased, the correlation of the chemical short-range order structure or the medium-range cluster size decreases. This suggests that the micro-inhomogeneous degree of the liquid Al–Ni–Ce alloys decreases with increasing temperature. As seen in table 1, the medium-range order cluster size of the liquid alloys is smaller than that of the amorphous alloys. It indicates that the medium-range order cluster grows to a larger size after being quenched to the amorphous state and the micro-inhomogeneous degree is increased. Although the medium-range order cluster is not stable in the solid state, the structural unit is stable and the medium-range order clusters grow to large sizes during rapid solidification. It may be due to the reduction of the redistribution of the constituent elements due to the increase in the quenching effects caused by the addition of Ce elements. According to the above discussion, the characteristic structural unit size

corresponding to the prepeak can be obtained from table 1. Its size is nearly 0.449 nm. During rapid solidification, the structural unit can be preserved to the amorphous state. Therefore during rapid solidification, the effect of the structural unit is like a large atom and enhances the glass forming ability of Al–Ni–Ce systems.

5. Conclusions

The medium-range order clusters are formed in the liquid state and the structural unit can be preserved to the amorphous state. The crystallization process followed by the amorphous Al₉₀Ni₅Ce₅ alloys is a two-stage one. The first stage corresponds to the precipitation of the fcc Al and in the second crystallization stage intermetallic compounds are formed. The structure corresponding to the prepeak is preserved, and even strengthened, during rapid solidification, but is not stable and decomposes at room temperature. Perhaps due to the increased quenching effects, the structure corresponding to the prepeak cannot be decomposed during rapid solidification. Therefore, the structural unit is like a large atom during rapid solidification, which is may be the reason for the high glass forming ability in Al–Ni–Ce systems.

Acknowledgment

This work was supported by the Natural Science Foundation of Shandong Province (NO.Y2000b02).

References

- [1] Sun W S, Quan M X and Li S L 1997 *J. Non-Cryst. Solids* **32** 6609
- [2] He Y, Poon S J and Shiflet G J 1988 *Science* **241** 1640
- [3] Inoue A, Ohtera K, Tsai A P and Masumoto T 1988 *J. Appl. Phys.* **27** 479
- [4] Kim Y K, Inoue A and Masumoto T 1991 *Mater. Trans. JIM.* **32** 331
- [5] Kim Y K, Inoue A and Masumoto T 1991 *Mater. Trans. JIM.* **32** 599
- [6] Kim Y K, Soh J R, Kim D K and Li H M 1998 *J. Non-Cryst. Solids* **242** 122
- [7] Inoue A, Ohtera K, Tsai A P and Masumoto T 1988 *J. Appl. Phys.* **27** L280
- [8] Matsubara E, Waseda Y, Inoue A, Ohtera H and Masumoto T 1989 *Z. Naturforsch. a* **44** 814
- [9] Hsieh H Y, Toby B H, He Y, Poon S J and Shiflet G J 1990 *J. Mater. Res.* **5** 2807
- [10] Hsieh H Y, Egami T, He Y and Poon S J 1991 *J. Non-Cryst. Solids* **135** 248
- [11] Mansour A N, Wrong C P and Brizzolara R A 1994 *Phys. Rev. B* **50** 12 401
- [12] Zhang Lin, Wu Youshi, Bian Xiufang, Lihui, Wang Weiming, Li Jingguo and Lun Ning 1999 *J. Phys.: Condens. Matter* **11** 7959
- [13] Li Q, Johnson E, Johanson A and Sarholt-kristensen L 1992 *J. Mater. Res.* **7** 2756
- [14] Wasada Y 1980 *The Structure of Non-Crystalline Materials* (New York: McGraw-Hill)
- [15] *International Tables for X-Ray Crystallography* 1974 (Birmingham: Kynoch)
- [16] Cromer D T and Mann J B 1967 *J. Chem. Phys.* **47** 1892
- [17] Qin Jingyu, Bian Xiufang, Sliuarenko S I and Wang Weimin 1998 *J. Phys.: Condens. Matter* **10** 1211
- [18] Egami T 1994 *Mater. Sci. Eng. A* **179–80** 17
- [19] Sokolov A P, Kisliuk A, Soltwisch M and Quitmann D 1992 *Phys. Rev. Lett.* **69** 1540
- [20] Dunlap R A, Yewondwossen M H, Srinivas V, Christie I A, Mehenty M E and Lloyd D J 1990 *J. Phys.: Condens. Matter* **2** 4315
- [21] Dzugutov M 1992 *Phys. Rev. A* **46** R2984
- [22] Elliott S R 1991 *Phys. Rev. Lett.* **67** T11
- [23] Massobrio C, Pasquarello A and Car R 1998 *Phys. Rev. Lett.* **80** 2342
- [24] Price D L, Moss S C, Reijers R, Saboung M-L and Susman S 1988 *J. Phys. C: Solid State Phys.* **21** L1069
- [25] Zhang Lin, Wu Youshi, Bian Xiufang, Lihui, Wang Weiming and Wu Si 1999 *J. Non-Cryst. Solids* **262** 169
- [26] Vateva E and Savova E 1991 *J. Non-Cryst. Solids* **192–3** 145